Lifetimes of bound excited states of the lanthanum negative ion and implications for laser cooling: Experiment and theory

C. W. Walter,[1] F. E. Vassallo,[1] J. Karls,[2] D. Leimbach,[2] D. Hanstorp,[2] J. E. Navarro Navarrete,[3] O. H. Lundgren,[2] M. K. Kristiansson,[3] M. Björkhage,[3] R. D. Thomas,[3] H. Zettergren,[3] H. T. Schmidt,[3] C. Cheung,[4] M. S. Safronova,[4] and N. D. Gibson[1]

[1]*Department of Physics and Astronomy, Denison University, Granville, Ohio 43023, USA*
[2]*Department of Physics, University of Gothenburg, Gothenburg 41296, Sweden*
[3]*Department of Physics, Stockholm University, Stockholm 10691, Sweden*
[4]*Department of Physics and Astronomy, University of Delaware, Newark, Delaware 19716, USA*

(Received 1 July 2025; accepted 3 October 2025; published 3 November 2025)

The negative ion of lanthanum has one of the richest bound-state spectra observed for an atomic negative ion and it has been proposed as a promising candidate for laser cooling, which has not yet been achieved for any negatively charged system. In the present study, radiative decays of low-lying excited states of La^- were experimentally investigated at the DESIREE cryogenic electrostatic ion-beam storage ring facility using state-selective photodetachment over storage times of up to 800 s. Independently, the transition rates for the relevant states were calculated using a high-precision hybrid theoretical approach. The measured lifetime of the lowest excited state of La^- ($^3F_3^e$) of 132(20) s agrees very well with the theoretical calculations and previous predictions. However, a puzzling discrepancy exists for the next-higher state $^3F_4^e$, with the experiments yielding a lifetime ∼4 times shorter than calculated, highlighting the challenges for this complex ion. The results provide valuable insights into the prospects for laser cooling La^-.

DOI: 10.1103/6641-mdhr

I. INTRODUCTION

Negative ions are interesting both for their importance in a variety of physical processes and for the essential insights they can provide into electron correlations. Because the extra electron in a negative ion is not bound to the neutral core by a net Coulomb force, their stability is crucially dependent on electron interactions. The shallow potential well in an atomic negative ion can typically support only a single bound-state configuration. Even in those few cases where a negative ion possesses multiple bound states, the states are very rarely of opposite parity. To date, electric dipole ($E1$) allowed absorption transitions between bound states have been directly observed in only four atomic negative ions: Os^- [1], Ce^- [2,3], La^- [4], and Th^- [5]. An important potential application of bound-bound transitions is in laser cooling, which has not yet been achieved for atomic negative ions. Finding even one negative ion that can be efficiently laser cooled could open up the ultracold regime to *all* negatively charged species through sympathetic cooling collisions, which could be used, for example, in cooling antiprotons for antimatter symmetry experiments [6,7].

Among atomic negative ions, that of lanthanum (La^-) is particularly intriguing because of its extraordinarily large number of bound states and its rich spectrum of bound-bound transitions. In 2009, O'Malley and Beck performed detailed relativistic configuration interaction (RCI) calculations that predicted La^- has seven even-parity bound states with configuration $[Xe]6s^25d^2$ and eight odd-parity bound states with configuration $[Xe]6s^25d6p$ [8]. Subsequently, in 2014, Walter *et al.* used resonant two-photon detachment spectroscopy to observe and identify 12 $E1$ transitions between bound states of La^-, confirming the general theoretical predictions and greatly refining the excitation energies for two of the even states and six of the odd states [4]. Kellerbauer and co-workers then made more detailed spectroscopic measurements for two of the bound-bound transitions [9–11]. In 2019, Lu *et al.* used slow electron velocity map imaging to measure the electron affinity of La (corresponding to the binding energy of the $La^-6s^25d^2\ ^3F_2^e$ ground state) as 557.553(25) meV and to determine the binding energies of all seven of the even bound states of La^- and one of the odd states [12]. Finally, in 2020, Blondel made a detailed analysis of the complete set of all available experimental data on La^- [4,9–12] to obtain a slightly revised La electron affinity of 557.546(20) meV, as well as optimized binding energies for 12 of the bound states of La^- [13].

The large number of $E1$ transitions in La^- suggests the exciting possibility of laser cooling this negative ion. Based on their theoretical calculations, O'Malley and Beck proposed the transition between the La^- $^3F_2^e$ ground state and $^3D_1^o$ excited state as an attractive option for laser cooling because the transition is relatively strong and the upper state decays with nearly 100% probability back to the initial ground state [14] (see Fig. 1). In 2018, Cerchiari *et al.* experimentally measured the $^3F_2^e \rightarrow {}^3D_1^o$ transition rate to be high $(4.90(50) \times 10^4\ s^{-1})$, and they performed additional theoretical calculations of the bound-state structure and transition rates [11]; these studies confirmed La^- as a promising candidate for laser cooling.

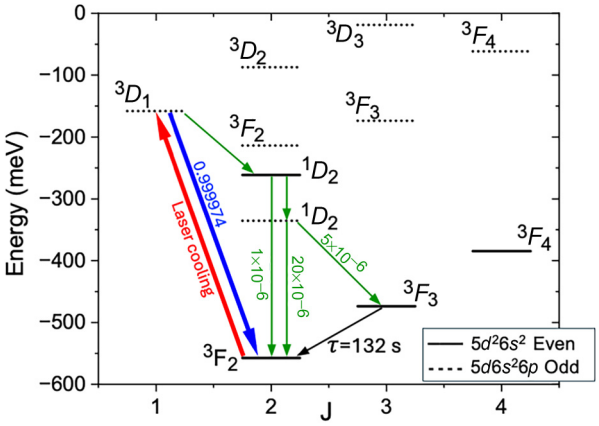

FIG. 1. Partial La^- energy level diagram relative to the La ground state showing the potential laser cooling transition $^3F_2^e \rightarrow {}^3D_1^o$ and the theoretical upper-state decay branching ratios calculated by Cerchiari *et al.* [11].

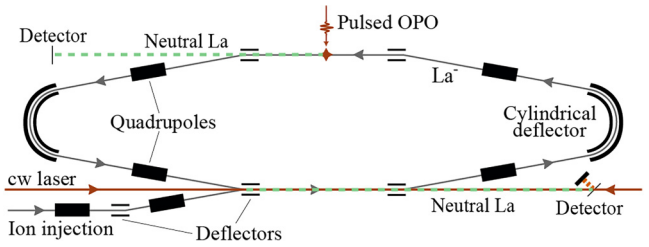

FIG. 2. Schematic of the apparatus used in the present experiments. La^- ions are injected and stored in the ring. A pulsed OPO beam interacts with the ions in a crossed-beam geometry on one side of the ring, and a cw laser beam interacts with the ions collinearly on the other side of the ring. Neutral La atoms produced by photodetachment travel straight forward from the interaction regions to hit neutral particle detectors on either side of the ring.

However, a potential complication for laser cooling La^- is the small predicted leakage from the closed cycle due to decay branching of the $^3D_1^o$ upper state via intermediate steps to the metastable $^3F_3^e$ fine structure excited state, which has a calculated radiative lifetime of ∼130 s [11,14]. Although branching to the $^3F_3^e$ state is expected to be very weak (only 5.2×10^{-6} [11]), a significant fraction of the ions could end up in this level after the many repeated transition cycles necessary for laser cooling if the lifetime is as long as theoretically predicted. However, the lifetime of $^3F_3^e$ has not yet been measured; therefore, it is important to experimentally test the calculations to assess whether it would be necessary to repump out of this "dark" state for a feasible laser cooling scheme.

In the present study, the radiative lifetimes of the two lowest bound excited states of La^- ($^3F_{3,4}^e$) were measured at the double electrostatic ion ring experiment (DESIREE) facility at Stockholm University [15,16]. In addition, the decay of a third, short-lived excited state was observed, but it could not be assigned to a particular level. State-selective photodetachment was used to monitor the populations of the ground state and excited ions in the ring for storage times of up to 800 s. Independently, the transition rates for the relevant states were calculated using a high-precision hybrid theoretical approach. The measured lifetimes of the $^3F_3^e$ and $^3F_4^e$ states are compared to the present and previous theoretical calculations, providing important information to assess the prospects for laser cooling La^- and yielding further insights into this complex ion.

II. EXPERIMENTAL METHOD AND RESULTS

The method for measuring radiative lifetimes of negative ion excited states at DESIREE has been described in detail previously [17–20]. In the present experiments, La^- ions were produced by a cesium sputter ion source (NEC SNICS II) using La powder in the cathode. Producing negative ions of lanthanides with a cesium sputter source is notoriously challenging because the lanthanide material tends to coat the ionizer, which reduces its efficiency due to the lowered work function of the surface [21]. Another challenge is that lanthanide cathodes tend to be rapidly destroyed in the sputtering process. To alleviate these problems in the present experiments, the voltage of 6 kV applied to the cathode was pulsed on for only ∼0.1 s at the start of each injection cycle and set to ground immediately afterward until the next cycle [22]. In this way, sputtering only took place for a small fraction of the overall experimental time, which greatly reduced the effect of ionizer poisoning and substantially prolonged the effective life of the cathode.

Following production in the source, the ions were accelerated to 10 keV, magnetically mass selected, and injected in bunches into the electrostatic storage ring (see Fig. 2). The high temperature of the source and energetic impact of cesium ions on the cathode surface produce La^- in a range of bound excited states; most of these states should radiatively decay during the ∼100-μs flight time to the ring based on the calculated lifetimes of La^- excited states [14]. The storage ring is contained in a vacuum chamber and kept at a cryogenic temperature of ∼13 K, which reduces the particle density of the rest gas in the UHV chamber to less than 10^4 cm^{-3}, facilitating effective storage of circulating ions for tens of minutes. After injection, the ion beam was exposed to light at several different wavelengths from a tunable pulsed optical parametric oscillator (OPO) (Ekspla NT342B) and a continuous-wave (cw) diode laser (CNI MIL-W-2796 nm) to selectively photodetach ions in different states to monitor the time evolution of the populations of ground state and excited ions for storage times of up to 800 s. Neutral atoms produced by photodetachment continued from the interaction regions straight out of the ring to hit neutral particle detectors situated on either side of the ring for signal counting [23]. A measurement cycle consisted of ion injection, storage for a preselected time interval during which neutral signal counts were collected from the detectors, and then dumping of the remaining ions from the ring after the storage time elapsed. This cycle was repeated many times to build up statistics.

State-selective photodetachment was used to monitor the time evolution of La^- state populations in the storage ring; see Fig. 3 for a schematic of the different photodetachment processes used in the present experiments. As noted previously, the electron affinity of La is 557.546(20) meV [12,13], which corresponds to a threshold wavelength for detachment

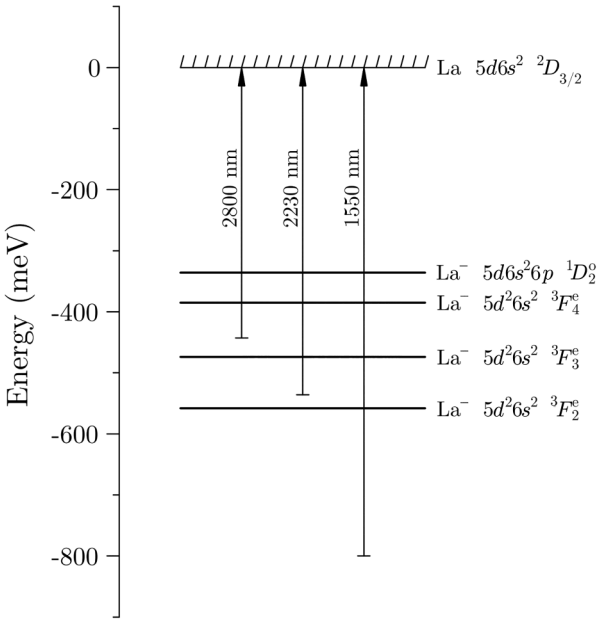

FIG. 3. La$^-$ energy level diagram showing the ground state and the three lowest excited states, together with the neutral La ground state. The arrows show the three wavelengths used in the present experiments to selectively monitor the ion state populations: 1550 nm produced by the pulsed OPO photodetaches all bound states of La$^-$, 2230 nm produced by the pulsed OPO photodetaches all of the excited states but not the ground state, and 2800 nm produced by the cw diode laser photodetaches all excited states except $^3F^e_3$.

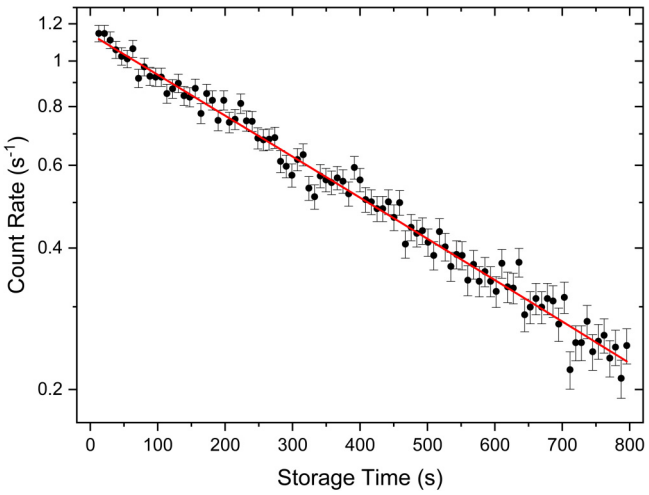

FIG. 4. Beam lifetime measured using the 1550-nm OPO, which can photodetach all bound states of La$^-$. The error bars on the signal rate data points represent one-sigma counting uncertainties. The neutral count rate data is fit with an exponential (solid red line) to determine the beam lifetime in the ring of 494(6) s.

from ground state La$^-$ $^3F^e_2$ of 2224 nm. The OPO tuned to 1550 nm (800 meV) was used to photodetach all bound states of La$^-$ in order to measure the overall ion-beam lifetime in the ring. The binding energy of the first excited state, $^3F^e_3$, is 473.605(28) meV [4,12,13]; to detach this state and all other excited states, but not the ground state, the OPO was tuned to 2230 nm (556 meV). Finally, the binding energy of the second excited state, $^3F^e_4$, is 384.677(33) meV [4,12,13]; the diode laser operating at 2800 nm (443 meV) was used to photodetach this state and all higher levels.

Two different arrangements for the interaction between photons and the ion beam were used to perform the present experiments (see Fig. 2). The 10-Hz pulsed OPO, with pulse duration of 5 ns and pulse energy of ∼1mJ, was directed perpendicular to the ion beam on one side of the ring over an interaction length of ∼5 mm. This arrangement allowed for arrival time gating of the detected neutral atoms to distinguish the photodetached signal from background counts. In contrast, the cw diode laser was aligned collinearly with the ion beam on the other side of the ring over a length of 70 cm, which yielded a much greater interaction volume to produce a sufficient photodetachment signal for feasible measurements of the neutral atom signal. The widths of the ion and laser beams in the interaction regions were ∼5 mm.

An important consideration for the overall ion-beam storage lifetime in the ring is the injected current; if the density of ions in the bunch is too high, the number of circulating ions decreases faster than the characteristic exponential decay due to ion-ion interactions [16]. Based on experience from experiments with ions of similar mass-to-charge ratio and energy, an ion-beam current of ∼0.2 nA (in the beginning of the measurement cycle) was used to avoid this effect [20].

The excellent vacuum in DESIREE enables the storage of beams of fragile negative ions for a very long time. Yet, the beam lifetime is finite due to collisions with background gas and/or random instabilities in their trajectories and should be measured and compensated for in the analysis. To accomplish this measurement, the overall ion-beam population was monitored using the OPO operating at 1550 nm, which can photodetach all bound states of La$^-$. The data for the count rate of photodetached neutrals as a function of time was fit with an exponential to determine the beam lifetime (see Fig. 4). The beam lifetime was measured to be 494(6) s, which is longer than the expected lifetimes of the excited states.

The initial excited-state lifetime measurements were performed with the cw laser operating at 2800 nm to photodetach La$^-$ $^3F^e_4$ and more weakly bound states. Two components were found in the decay curve, indicating the presence of a short-lived state (lifetime ∼0.2 s) and a longer-lived state (lifetime ∼30 s). Based on comparison to the calculated lifetimes of La$^-$ excited states by O'Malley and Beck [14] and by Cerchiari *et al.* [11], the longer-lived state can be uniquely identified as $^3F^e_4$, since it is the only excited state accessible for photodetachment at this wavelength with a calculated lifetime of more than 2 s. However, the identity of the short-lived state is not clear, as none of the excited states are predicted to have lifetimes within a factor of 5 shorter or longer than the observed decay lifetime.

In order to rapidly build up statistics on the short-lived state, a series of injection cycles with a storage time of only 2 s were made; a typical count-rate decay curve collected in this manner is shown in Fig. 5. The observed decay rate, determined by fitting the data with exponential functions, was found to be weakly dependent on the laser power due to depletion of the excited-state ions by photodetachment. Therefore,

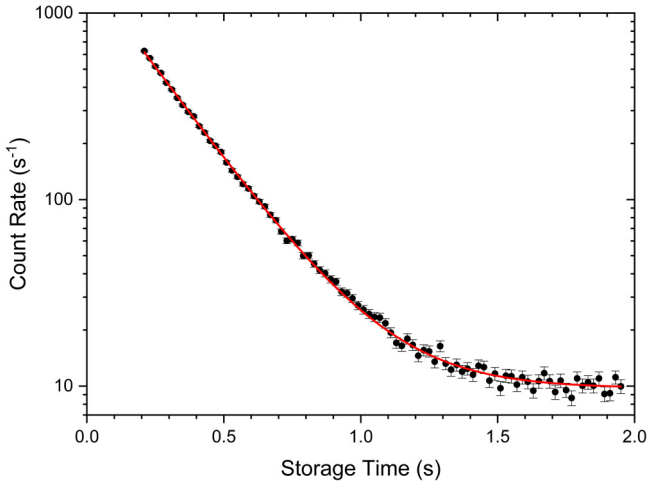

FIG. 5. Neutral atom count-rate decay curve over the first 2 s after injection obtained with the 2800-nm cw laser with a power of 3 mW measured after the chamber. The rapid decrease over the first ∼1 s is due to decay of the short-lived state, whereas the more gradual decrease at later times is due to decay of the much longer-lived $^3F_4^e$ state. The data is fit with a double-exponential function (solid red line) to obtain the decay rate for the short-lived excited state at this laser power of ∼5 s^{-1}, which corresponds to an effective lifetime of ∼0.2 s for this data set.

in order to obtain the natural lifetime of the state, lifetime measurements were collected over a range of laser powers. The measured decay rate was then graphed as a function of laser power in a Stern-Volmer plot. Two series of experiments were performed with different laser–ion-beam alignments; extrapolating the decay rate with linear fits to zero laser power gave very similar intercepts for the two measurement series (see Fig. 6). The weighted average of the fits yielded the natural lifetime of the short-lived state to be 0.22(3) s.

Following characterization of the short-lived state, experiments were performed with longer storage times of up to 800 s

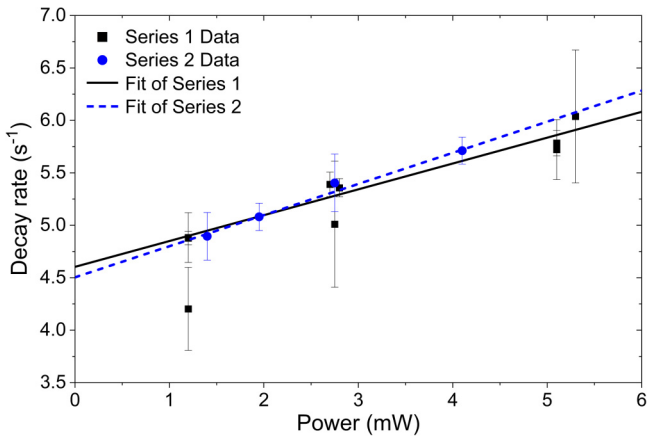

FIG. 6. Stern-Volmer plot of the measured decay rate of the short-lived state as a function of laser power through the chamber. Two series of measurements were performed with different laser–ion-beam alignments. The weighted average of the linear fits extrapolated to zero power yields the natural lifetime of the state to be 0.22(3) s.

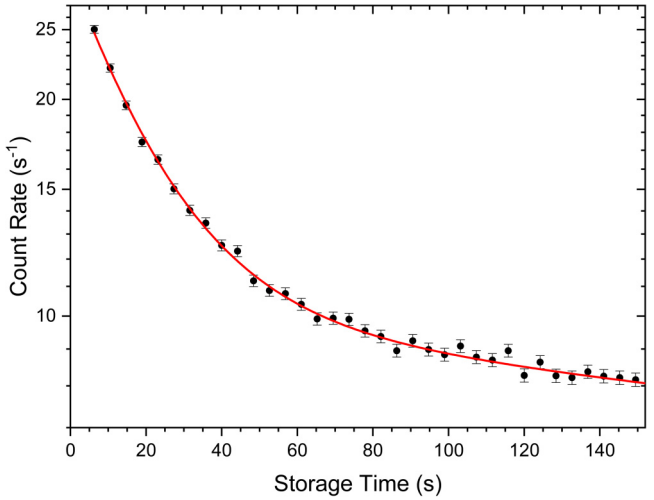

FIG. 7. Neutral atom count-rate decay curve from 5 to 145 s after injection obtained with the 2800-nm cw laser with a power of 1.95 mW measured after the chamber. The rapid decrease over the first ∼80 s is due to radiative decay of $^3F_4^e$, while the later time slow decay is due to the overall loss of ions in the stored beam. The data is fit with a double-exponential function (solid red line) with slow component fixed at the previously determined beam lifetime of 494(6) s in order to obtain the decay rate for $^3F_4^e$ at this laser power of 0.043 s^{-1}, which corresponds to an effective lifetime of 22 s for this data set.

to investigate the decay of the $^3F_4^e$ ions with the 2800-nm cw laser used for photodetachment. A typical decay curve measured for $^3F_4^e$ is shown in Fig. 7. The observed decay rate was again found to depend on the laser power due to photodetachment depletion of the excited state, so data were collected at different laser powers in two series of experiments with different laser–ion-beam alignments. The Stern-Volmer plot of the measured decay rate of $^3F_4^e$ as a function of laser power is shown in Fig. 8. The second measurement series had a higher overlap of the laser and ion beams, leading to substantially greater photodetachment and a steeper slope on the Stern-Volmer plot; however, the intercepts of the fits to the two data series closely agree, as was to be expected since the extrapolation of the decay rate to zero laser power should not depend on the beam overlap. The effective lifetime of the $^3F_4^e$ excited state was determined from the Stern-Volmer plot to be 30(5) s. Although this is an order of magnitude shorter than the beam lifetime of 494 s, the effective lifetime is still slightly affected by the overall loss of stored ions throughout the cycle. Taking into account this loss, the natural lifetime is obtained by $1/\tau_{\text{natural}} = 1/\tau_{\text{effective}} - 1/\tau_{\text{beam}}$. The natural lifetime of $^3F_4^e$ was determined to be 32(5) s.

The lifetime of the lowest excited state, $^3F_3^e$, was measured using the pulsed OPO tuned to 2230 nm, which can photodetach all of the excited states of La^- but not the ground state. In this case, there was not significant photodetachment depletion of the ions during the 800-s storage time, because of the OPO's low repetition rate, short pulse duration, and small interaction length with the ion beam in the crossed-beam arrangement. A typical decay curve is shown in Fig. 9. The time evolution of the signal in this case is due to photodetachment from two different long-lived populations ($^3F_3^e$ and $^3F_4^e$), as

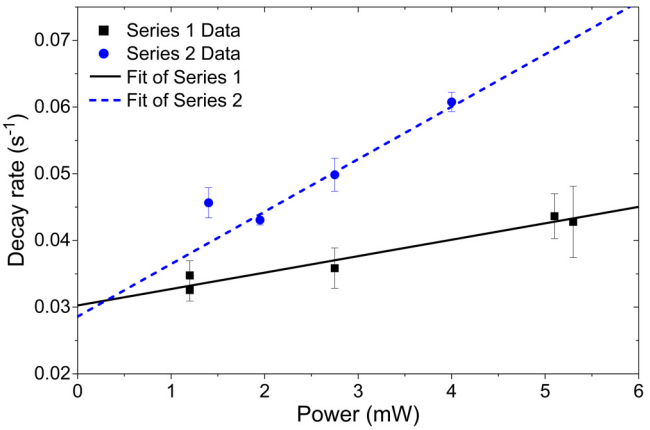

FIG. 8. Stern-Volmer plot of the measured decay rate of La^- $^3F_4^e$ ions as a function of laser power through the chamber. Two series of measurements were performed with different laser–ion-beam alignments. Series 2 had higher overlap of the beams and thus stronger photodetachment depletion leading to a steeper slope; however, the intercepts of the fit lines for the two series closely agree, as expected. Linear fits extrapolated to zero power yield an effective lifetime of 30(5) s. After accounting for the beam lifetime, the natural lifetime of $^3F_4^e$ was determined to be 32(5) s.

well as the overall loss of ions in the beam throughout the storage time; thus, there are three contributions to the decay curve. Several different analysis methods were employed for fitting the data to extract the $^3F_3^e$ lifetime, including allowing the $^3F_4^e$ lifetime either to vary in the fit or to be fixed at the previously determined value of 32(5) s. Although there were not large differences between different approaches, the most consistent method was found to be fitting only the data after 120 s to allow time for decay of effectively all $^3F_4^e$ ions, leaving all remaining excited ions in the beam only in the $^3F_3^e$

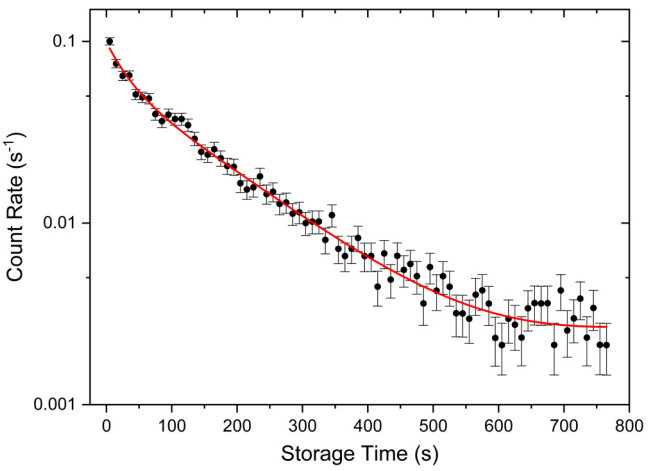

FIG. 9. Neutral atom count-rate decay curve obtained with the 2230-nm OPO, which can photodetach all excited states of La^-. A triple-exponential fit (solid red line) to the data reveals three distinct population evolutions: The rapid decrease in count rate over the first ∼60 s is due to decay of $^3F_4^e$ ions [lifetime 32(5) s]; the slower drop from 60 s to ∼500 s is due to decay of $^3F_3^e$ ions [lifetime 132(20) s], and the very slow decrease after 500 s is due to the overall loss of ions in the stored beam [beam lifetime 494(6) s].

state. This later time data was fit with a double-exponential function representing the $^3F_3^e$ decay (which had a variable lifetime) and the overall ion beam decay [set at the fixed beam lifetime previously determined to be 494(6) s]. The natural lifetime of $^3F_3^e$ was determined to be 132(20) s.

III. THEORY

Independently from the experiments, theoretical calculations of the relevant La^- excited-state decay rates were performed. We consider La^- as a system with four valence electrons and a $[1s^2 \ldots 5p^6]$ closed core. The computations of the lifetimes are performed in the framework of CI + all-order [24] with the pCI package [25], following our previous computations [11]. We begin by solving the Dirac-Hartree-Fock equations for the core electrons, and then construct the $6s$, $5d$, $4f$, $6p$, $7s$, and $7p$ orbitals in the frozen-core potential. The remaining virtual orbitals are formed using 40 B-splines of order 7. The final basis set is constructed on a radial grid constrained to a spherical cavity of $R = 60$ a.u., including orbitals with principal quantum number n up to 35 for seven partial waves ($l_{\max} = 6$). The Coulomb and Breit interactions were included on the same footing for all calculations.

In the CI + all-order approach, we use the linearized coupled-cluster method to construct an effective Hamiltonian describing core-core and core-valence correlations, and then use the CI method to construct the wave function as a linear combination of all possible many-electron states with a given angular momentum J and parity, $\Psi_J = \sum_i c_i \Phi_i$. The final wave function includes configurations obtained by allowing single and double excitations from the $6s^2 5d^2$ configuration to all orbitals up to $n = 24$ for the *spdfg* orbital angular momentum partial waves. The energies and wave functions are determined by diagonalizing the effective Hamiltonian, then subsequently used to compute the relevant matrix elements, transition rates, and lifetimes of the $^3F_{3,4}^e$ states.

The $^3F_3^e$ and $^3F_4^e$ lifetimes are dominated by magnetic dipole ($M1$) transitions to the $^3F_2^e$ ground state and $^3F_3^e$ state, respectively. We found that the $^3F_4^e \rightarrow {}^3F_2^e$ electric quadrupole ($E2$) transition had a negligible contribution to the $^3F_4^e$ lifetime, since its rate of 2.5×10^{-8} s^{-1} is 5 orders of magnitude smaller than the $^3F_4^e \rightarrow {}^3F_3^e$ $M1$ transition rate of 7.41×10^{-3} s^{-1}. We obtained a lifetime of 131 s for the $^3F_3^e$ state and 135 s for the $^3F_4^e$ state.

IV. DISCUSSION

The results for the measured lifetimes of La^- excited states are summarized in Table I together with the present and previous theoretical calculations. The first theoretical calculations of the lifetimes of excited states of La^- were performed by O'Malley and Beck in 2010 using the relativistic configuration interaction method [14]. Their calculations gave a $^3F_3^e$ lifetime of 260 s for the predominantly $M1$ decay to the ground state $^3F_2^e$. However, their calculated $^3F_3^e \rightarrow {}^3F_2^e$ transition energy of 67 meV is significantly smaller than the subsequently measured value of 83.94(2) meV [4,12,13]. The $M1$ transition rate scales inversely as the third power of the energy gap; therefore, O'Malley and Beck's calculated lifetime should

TABLE I. Measured and calculated lifetimes of La^- excited states in seconds.

State	Present experiment	Present theory	O'Malley and Beck [14]	Cerchiari *et al.* [11]
$^3F_3^e$	132(20)	131	132[a]	132
$^3F_4^e$	32(5)	135	134[a]	
Short-lived	0.22(3)			

[a]Rescaled using the measured transition energies; see text.

be rescaled using the experimental transition energy, which yields a $^3F_3^e$ lifetime of 132 s. More recently, theoretical calculations of La^- excited-state lifetimes were carried out by Cerchiari *et al.* using a larger-scale hybrid configuration interaction plus all-order coupled-cluster method [11]. Their calculated $^3F_3^e$ lifetime using the experimental energy gap was also 132 s [11]. The present theoretical calculations, using a very slightly different basis set than that of Ref. [11], yield a lifetime of 131 s. Our experimentally measured lifetime for $^3F_3^e$ of 132(20) s agrees very closely with the theoretical values, verifying the accuracy of the calculations for radiative decay of the $^3F_3^e$ excited state.

The present results directly bear on the question of the feasibility of laser cooling of La^- via the $^3F_2^e \rightarrow {}^3D_1^o$ transition. As discussed previously, there is a small leakage from the nearly closed cycle of this transition due to decay of the upper state via intermediate steps to the $^3F_3^e$ metastable state. Although this branching is predicted to be very weak (5.2×10^{-6} [11]), a significant population may build up in the $^3F_3^e$ state, given its presently measured lifetime of 132 s. Thus, as suggested by Cerchiari *et al.* [11], effective laser cooling would likely require repumping out of the $^3F_3^e$ "dark" state.

Turning now to the second excited state, the first theoretical calculations for radiative decay of $^3F_4^e$ were performed by O'Malley and Beck [14]. Their original calculations gave a lifetime of 300 s for this state, with the primary decay channel being the $M1$ transition to $^3F_3^e$. However, their calculated $^3F_4^e \rightarrow {}^3F_3^e$ transition of 68 meV for this transition is significantly smaller than the later established experimental value of 88.93(3) meV [4,12,13]. Rescaling O'Malley and Beck's calculated lifetime using the experimental energy gap gives a $^3F_4^e$ lifetime of 134 s. Our present theoretical calculations yield a lifetime for this state of 135 s, closely agreeing with the previous calculations. However, our measured lifetime for $^3F_4^e$ of 32(5) s is about 4 times shorter than the calculated values. The reason for the discrepancy is unclear, especially given the close agreement between theory and experiment for the lifetime of the $^3F_3^e$ state. For both states, the dominant decay mode is calculated to be $M1$ decay to the next-lower state. $^3F_4^e$, however, can also decay by $E2$ radiation to the ground state $^3F_2^e$. As noted previously, the $E2$ decay channel is calculated to be 5 orders of magnitude weaker than the $M1$ channel, therefore it appears unlikely that the difference in the $^3F_4^e$ lifetime is due to the additional decay channel of the state. This puzzling discrepancy highlights the challenges in determining the properties of this complex ion and the need for both experimental and theoretical investigations.

Finally, the origin of the early time signal with a measured lifetime of 0.22(3) s is yet to be identified. Useful information is provided by the observed photodetachment count rate, which is significantly larger for this state by a factor of $\sim$100 than for the $^3F_4^e$ state (see Fig. 5). This much higher signal suggests that it is due to photodetachment from an odd-parity La^- state of configuration $6s^2 5d 6p$, which will have a much greater photodetachment cross section to the neutral La $6s^2 5d$ ground state than will an even-parity state ($6s^2 5d^2$), due to s-wave detachment near threshold as opposed to p-wave. Therefore, an obvious candidate is the lowest odd-parity state, $^1D_2^o$. Note that in the La^- photodetachment spectrum obtained by Walter *et al.*, the s-wave threshold from $^1D_2^o$ appeared quite prominently (see Figs. 2 and 3 of Ref. [4]). However, the energy-rescaled calculated lifetimes of $^1D_2^o$ are only 0.0038 and 0.0045 s from O'Malley and Beck [14] and Cerchiari *et al.* [11], respectively. The present calculations obtain a lifetime for this state of 0.0049 s, which is on the same order as the previous predictions. The theoretical lifetimes of $^1D_2^o$ are a factor of $\sim$50 times shorter than that measured for the short-lived state, making it unlikely to be the state solely responsible for the observed early time signal. It may be that the observed early signal is due to a decay cascade from higher-lying states in the initial ion beam to the $^1D_2^o$ state, from which photodetachment takes place with a high cross section. Further experimental and theoretical investigations would be needed to fully identify the origin of the early time signal.

V. CONCLUSIONS

In summary, the radiative lifetimes of the two lowest excited states of La^- have been measured and theoretically calculated. The first excited state, $^3F_3^e$, was found to have a lifetime of 132(20) s, in excellent agreement with the theoretical calculations. However, the lifetime of the next excited state, $^3F_4^e$, was measured to be 32(5) s, which is a factor of $\sim$4 shorter than the calculated value. Furthermore, a short-lived excited state of lifetime 0.22(3) s was observed, but it has not yet been possible to identify the origin of this photodetachment signal. The present results highlight both successes and remaining challenges for fully understanding this complex negative ion.

The present measurements confirm the long lifetime predicted for the $^3F_3^e$ state. This state is a loss channel for the proposed laser cooling cycling transition; thus, it would most likely require repumping out of this "dark" state to depopulate it for efficient laser cooling. Despite this experimental complication, La^- remains a promising candidate for laser cooling applications with negative ions.

ACKNOWLEDGMENTS

The experiments in this work were performed at the Swedish National Infrastructure, DESIREE (Swedish Research Council Contracts No. 2017-00621, No. 2021-00155,

and No. 2023-00170). This work was supported in part by U.S. NSF Grants No. PHY-2110444, No. PHY-2409073, and No. PHY-2309254, and Office of Naval Research Grant No. N000142512105. H.Z., H.T.S., and D.H. thank the Swedish Research Council for individual project grants (with Contracts No. 2020-03437, No. 2022-02822, and No. 2020-03505), and the Knut and Alice Wallenberg foundation for Project Grant No. 2024.0134. F.E.V. received partial support from Denison University's William G. & Mary Ellen Bowen Research Endowment. The calculations in this work were done through the use of Information Technologies resources at the University of Delaware, specifically the high-performance Caviness and DARWIN computer clusters.

DATA AVAILABILITY

The data that support the findings of this article are not publicly available. The data are available from the authors upon reasonable request.

[1] R. C. Bilodeau and H. K. Haugen, Phys. Rev. Lett. **85**, 534 (2000).
[2] C. W. Walter, N. D. Gibson, C. M. Janczak, K. A. Starr, A. P. Snedden, R. L. Field, III, and P. Andersson, Phys. Rev. A **76**, 052702 (2007).
[3] C. W. Walter, N. D. Gibson, Y. G. Li, D. J. Matyas, R. M. Alton, S. E. Lou, R. L. Field, III, D. Hanstorp, L. Pan, and D. R. Beck, Phys. Rev. A **84**, 032514 (2011).
[4] C. W. Walter, N. D. Gibson, D. J. Matyas, C. Crocker, K. A. Dungan, B. R. Matola, and J. Rohlén, Phys. Rev. Lett. **113**, 063001 (2014).
[5] R. Tang, R. Si, Z. Fei, X. Fu, Y. Lu, T. Brage, H. Liu, C. Chen, and C. Ning, Phys. Rev. A **103**, 042817 (2021).
[6] A. Kellerbauer and J. Walz, New J. Phys. **8**, 45 (2006).
[7] A. Kellerbauer, M. Amoretti, A. S. Belov, G. Bonomic, I. Boscolo, R. S. Brusa, M. Buchner, V. M. Byakov, L. Cabaret, C. Canali, C. Carraro, F. Castelli, S. Cialdi, M. de Combarieu, D. Comparat, G. Consolati, N. Djourelov, M. Doser, G. Drobychev, A. Dupasquier *et al.*, Nucl. Instrum. Methods Phys. Res. Sect. B **266**, 351 (2008).
[8] S. M. O'Malley and D. R. Beck, Phys. Rev. A **79**, 012511 (2009).
[9] A. Kellerbauer, G. Cerchiari, E. Jordan, and C. W. Walter, Phys. Scr. **90**, 054014 (2015).
[10] E. Jordan, G. Cerchiari, S. Fritzsche, and A. Kellerbauer, Phys. Rev. Lett. **115**, 113001 (2015).
[11] G. Cerchiari, A. Kellerbauer, M. S. Safronova, U. I. Safronova, and P. Yzombard, Phys. Rev. Lett. **120**, 133205 (2018).
[12] Y. Lu, R. Tang, X. Fu, and C. Ning, Phys. Rev. A **99**, 062507 (2019).
[13] C. Blondel, Phys. Rev. A **101**, 016501 (2020).
[14] S. M. O'Malley and D. R. Beck, Phys. Rev. A **81**, 032503 (2010).
[15] R. D. Thomas, H. T. Schmidt, G. Andler, M. Björkhage, M. Blom, L. Brannholm, E. Backstrom, H. Danared, S. Das, N. Haag, P. Hallden, F. Hellberg, A. I. S. Holm, H. A. B. Johansson, A. Kallberg, G. Kallersjo, M. Larsson, S. Leontein, L. Liljeby, P. Lofgren *et al.*, Rev. Sci. Instr. **82**, 065112 (2011).
[16] H. Schmidt, R. Thomas, M. Gatchell, S. Rosén, P. Reinhed, P. Löfgren, L. Brännholm, M. Blom, M. Björkhage, E. Bäckström *et al.*, Rev. Sci. Instrum. **84**, 055115 (2013).
[17] E. Bäckström, D. Hanstorp, O. M. Hole, M. Kaminska, R. F. Nascimento, M. Blom, M. Björkhage, A. Källberg, P. Löfgren, P. Reinhed, S. Rosén, A. Simonsson, R. D. Thomas, S. Mannervik, H. T. Schmidt, and H. Cederquist, Phys. Rev. Lett. **114**, 143003 (2015).
[18] K. C. Chartkunchand, M. Kamińska, E. K. Anderson, M. K. Kristiansson, G. Eklund, O. M. Hole, R. F. Nascimento, M. Blom, M. Björkhage, A. Källberg, P. Löfgren, P. Reinhed, S. Rosén, A. Simonsson, R. D. Thomas, S. Mannervik, V. T. Davis, P. A. Neill, J. S. Thompson, D. Hanstorp *et al.*, Phys. Rev. A **94**, 032501 (2016).
[19] M. K. Kristiansson, S. Schiffmann, J. Grumer, J. Karls, N. de Ruette, G. Eklund, V. Ideböhn, N. D. Gibson, T. Brage, H. Zettergren, D. Hanstorp, and H. T. Schmidt, Phys. Rev. A **103**, 062806 (2021).
[20] M. K. Kristiansson, J. Karls, N. D. Gibson, D. Hanstorp, H. T. Schmidt, and C. W. Walter, Phys. Rev. A **105**, L010801 (2022).
[21] R. Middleton, *A Negative-Ion Cookbook* (University of Pennsylvania, Philadelphia, 1990).
[22] J. Blahins, T. Leopold, A. Apsitis, U. Berzins, A. Ubelis, J. Rohlén, D. Lu, and D. Hanstorp, Rev. Sci. Instrum. **91**, 023322 (2020).
[23] J. Warbinek, D. Leimbach, D. Lu, K. Wendt, D. J. Pegg, A. Yurgens, D. Hanstorp, and J. Welander, Appl. Phys. Lett. **114**, 061902 (2019).
[24] M. S. Safronova, M. G. Kozlov, W. R. Johnson, and D. Jiang, Phys. Rev. A **80**, 012516 (2009).
[25] C. Cheung, M. G. Kozlov, S. G. Porsev, M. S. Safronova, I. I. Tupitsyn, and A. I. Bondarev, Comput. Phys. Commun. **308**, 109463 (2025).